

1 **Comment on “Pressure-to-Depth Conversion Models for Metamorphic Rocks: Derivation**  
2 **and Applications”**

3  
4 Dazhi Jiang<sup>1,2</sup> ([djiang3@uwo.ca](mailto:djiang3@uwo.ca))

5 <sup>1</sup>Department of Earth Sciences, Western University, London, Canada

6 <sup>2</sup>Department of Geology, Northwest University, Xi'an, China

7  
8 **Abstract:** Bauville and Yamato (2021, G-cubed, <https://doi.org/10.1029/2020GC009280>)  
9 propose model-based methods to convert metamorphic pressures to depths based on the claim  
10 that pressure data from global (ultra)high-pressure rocks challenge the lithostatic assumption and  
11 support their model which invokes excessive overpressures. It is argued here that the opposite is  
12 true: Natural pressure data are fully consistent with the lithostatic assumption. They reflect  
13 selection of (ultra)high-pressure rocks by accessibility and preservation. The data are however  
14 inconsistent with the model predictions of Yamato and Brun (2017, Nature Geoscience 10, 46-  
15 50) and Bauville and Yamato (2021). Furthermore, their model requires critical assumptions that  
16 are not justified by the principles of rock mechanics and unsupported by microstructures from  
17 (U)HP rocks.

18

19 **1. Introduction**

20 Yamato and Brun (2017) and Bauville and Yamato (2021) claim that metamorphic pressures  
21 from global (ultra)high-pressure ((U)HP) rocks challenge the lithostatic pressure assumption but  
22 support their model that invokes excessive overpressures. Bauville and Yamato (2021) propose  
23 methods to convert metamorphic pressure data to depths on the basis of the Yamato and Brun  
24 model and its development. The purpose of this comment is threefold. First, I contest their  
25 interpretation of the natural pressure data and argue that the data are fully consistent with and  
26 better explained by the current interpretations based on the lithostatic assumption. Second, I  
27 point out that their model requires critical assumptions that are not justified by the principles of  
28 rock mechanics and unsupported by microstructures of (U)HP rocks. Finally, I question some  
29 concepts and derivations in Bauville and Yamato (2021), related to finite strain deformation,  
30 stress rotations, and the Mohr-Coulomb rheology.

31 **2. Do Pressure Data from (U)HP Rocks Challenge the Lithostatic Assumption and**  
32 **Support a Mechanic Model Invoking Excessive Overpressures?**

33 The mineral assemblages of (U)HP rocks commonly record a ‘peak’ pressure ( $P_p$ ), which  
34 is commonly interpreted by researchers to represent the maximum depth of rock burial, and a  
35 lower ‘retrograde’ pressure ( $P_r$ ) interpreted to represent the depth of the initial isothermal  
36 decompression (Ernst et al., 2007; Hacker and Gerya 2013; Powell and Holland, 2010). The  
37 pressure drop,  $\Delta P = P_p - P_r$ , thus corresponds to the amount of exhumation attained by the  
38 isothermal decompression. This interpretation assumes that  $P_p$  and  $P_r$  are approximately  
39 lithostatic (lithostatic assumption, hereafter). In reality, both  $P_p$  and  $P_r$  may deviate from the  
40 lithostatic values, but the magnitude of deviation is limited by the rock strength, which is likely  
41 less than hundreds of MPa for the time scale relevant for (U)HP metamorphism and far below  
42 the GPa level lithostatic pressure (e.g., Jiang and Bhandari 2018).

43 The pressure data from global (U)HP rocks as compiled in Bauville and Yamato (2021)  
44 are replotted in the  $P_p$  vs  $\Delta P$  space (Fig.1A) and in the  $P_p$  vs  $P_r$  space (Fig.1C). Yamato and  
45 Brun (2017) claim that the linear relation between  $P_p$  and  $\Delta P$  challenges the lithostatic  
46 assumption but supports their model that invokes excessive overpressures. They propose that  
47  $\Delta P$  may be due to a switch in stress regime, from compression to extension, at the same depth  
48 without actual ascent of the rocks. Bauville and Yamato (2021) argue that there is a linear  
49 dependence of  $P_r$  on  $P_p$  that requires their model to explain.

50 Let us first examine the plot in Fig.1A carefully and see if the assumption that  $P_p$  and  $P_r$   
51 are lithostatic will lead to great difficulty.

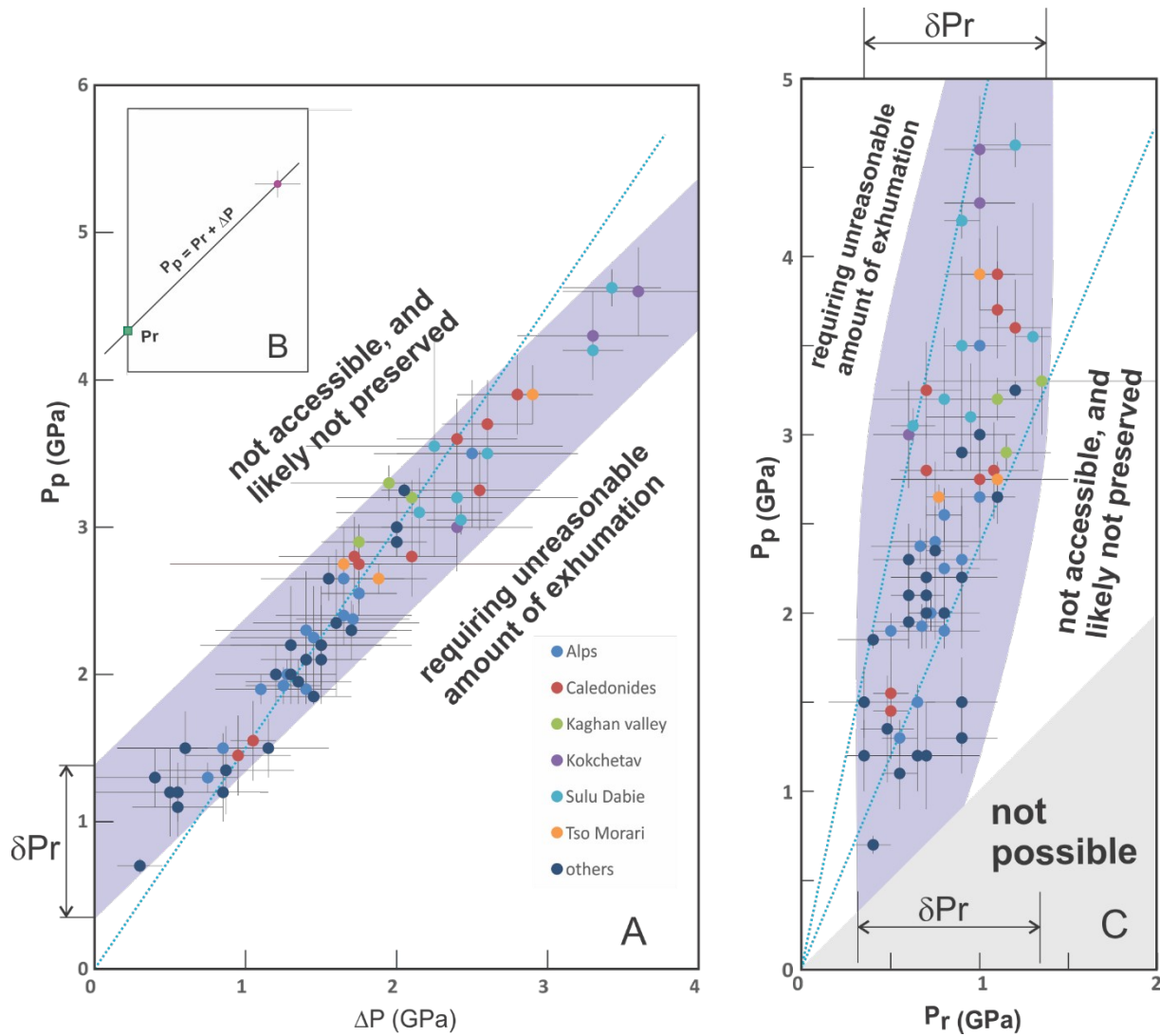
52 As  $P_p$ ,  $P_r$ , and  $\Delta P$  are related by  $P_p = \Delta P + P_r$ , for each data point in Fig.1A, one can  
53 draw a line of unit slope passing the data point and the intercept of the line on the vertical axis is

54 the corresponding  $P_r$  (Fig.1B). Considering this for all data points in the set, one realizes that all  
 55  $P_r$  are clustered within a narrow strip ( $\delta P_r$ , purple-shaded in Fig.1A) between  $\sim 0.3$  and  $1.3$  GPa.  
 56 The trend for all the data, having a linear regression fit of  $P_p = 1.17\Delta P + 0.52$ , is because of the  
 57 limited range in  $P_r$ . With the lithostatic assumption,  $\delta P_r$  corresponds to depths between  $\sim 12$  and  
 58  $50$  km. Thus, Fig.1A suggests that although (U)HP rocks in the current dataset were formed over  
 59 a great pressure range ( $1$  to over  $4$  GPa), corresponding to  $35$  km and  $>140$  km depth difference,  
 60 they were exhumed during the isothermal decompression stage to the limited depth range of  $\sim 12$   
 61 and  $50$  km. This depth range may simply represent the interval where (U)HP rocks are preserved  
 62 after formation at deeper levels *and* are accessible to our observations. The ultra-high pressure  
 63 assemblages with  $P_r > \sim 1.3$  GPa may not have been preserved and, if preserved, may still be buried  
 64 and not accessible for observation yet. Thus, the linear trend of the data simply reflects natural  
 65 selection of (U)HP rocks by accessibility and preservation.

66 Yamato and Brun (2017) claim that the linear relation showing in Fig.1A challenges the  
 67 lithostatic assumption but supports their model prediction of  $P_p = 1.5\Delta P$  (the dashed blue line).  
 68 However, the linear regression fit of the data has a slope of  $1.17$ , significantly shallower than  
 69 the predicted  $1.5$ , and a significant positive intercept of  $0.52$  as opposed to the model-predicted  
 70 small negative intercept (Yamato and Brun, 2017).

71 Perhaps noticing the above discrepancy between data and prediction, Bauville and  
 72 Yamato (2021) used the  $P_p$  vs  $P_r$  plot instead. In the plot of the same data here (Fig.1C), I have  
 73 used an equal scale for  $P_r$  and  $P_p$  to avoid distortion of line slopes. Fig.1C is also fully  
 74 compatible with the lithostatic assumption. One should note that although in the lithostatic  
 75 interpretation  $P_p$  and  $P_r$  represent two events at different depths, the distribution  $P_p$  vs  $P_r$  are  
 76 *not* totally random in space because of the following constraints. First, by definition all data must  
 77 plot above the  $P_p = P_r$  line (grey-shaded area in Fig.1C). Second, as (U)HP rocks are formed in  
 78 low-temperature and high-pressure settings, they must be exhumed, shortly after formation  
 79 (Ernst et al., 2007), to shallower depths (corresponding to  $\delta P_r$  in Fig.1A and C) so that the  
 80 (U)HP assemblages are preserved. Direct geological observations are also constrained by the  
 81 accessibility of rock exposures. The  $\delta P_r$  interval is consistent with accessible range for direct  
 82 observations. Thus, a greater  $P_p$  must in general be associated with a greater  $\Delta P$  as shown by  
 83 Fig.1A. Although exhumation rate varies and may be as fast as the subduction rate (e.g., Rubatto  
 84 and Hermann, 2001; Parrish et al., 2006), the maximum amount of stage 1 exhumation is always  
 85 limited by the duration of the exhumation multiplied by the rate. This means that an extremely  
 86 low  $P_r$  (like  $0.5$  GPa) associated with very high  $P_p$  (like  $4.0$  GPa) is unlikely, as such a  $P_p$  and  $P_r$   
 87 pair requires an unreasonable amount of exhumation in stage 1 (Fig.1C). With the above

88 constraints considered, the distribution of  $P_p$  and  $P_r$  in Fig.1C is fully consistent with  $P_r$  being  
 89 independent of  $P_p$ .



90

91 Figure 1: Metamorphic pressure data from global (U)HP rocks. (A): Plot of  $P_p$  vs  $\Delta P$  of data  
 92 with error bars. Purple shaded region represents the narrow strip of  $\delta P_r$  between 0.3 and 1.3  
 93 GPa. The blue dashed line is the model-predicted relation ( $P_p = 1.5\Delta P$ ) of Yamato and Brun  
 94 (2017). (B) Each data point corresponds to a  $P_r$  through the definition relation  $P_p = \Delta P + P_r$ . (C):  
 95 The same data with error bars plotted in the  $P_p$  vs  $P_r$  space. The upper bound of the grey-shaded  
 96 area is given by  $P_p = P_r + \delta P_r$ .  $\delta P_r$  corresponds to that in (A). The two blue dashed lines define the  
 97 fan area of Bauville and Yamato (2021). Purple shaded region outlines the domain (U)HP rocks

98 are preserved and accessible. The data are compiled in Bauville and Yamato (2021). See text for  
99 more detail.

100

101 The argument of Bauville and Yamato (2021) that Fig.1C shows a linear dependence of

102  $P_r$  on  $P_p$  is rather far-fetched. The authors have to first exclude data points with  $\frac{P_p}{P_r} < 2.4$  as  
103 “outliers” and then propose that the fan area with  $2.4P_r < P_p < 4.8P_r$  (the two dashed blue lines in  
104 Fig.1C) represents the “linear dependence” of  $P_r$  on  $P_p$ . If all data points were included and the  
105 error bars of  $P_r$  also considered, the fan would have a much wider angle, essentially covering  
106 almost the entire space except the grey-shaded area in Fig.1C.

107

### 108 3. Model Assumptions

109 The model proposed by Yamato and Brun (2017) which was used and elaborated by  
110 Bauville and Yamato (2021) requires the following assumptions: 1) the rock rheology follows a  
111 Mohr-Coulomb plasticity or a Byerlee’s frictional behavior, 2) the stress state is close to or at the  
112 yield state, and 3) the stress state is Andersonian.

113 None of these assumptions can be well justified for (U)HP metamorphism. First, Mohr-  
114 Coulomb plasticity and Byerlee’s frictional behaviors are the rheological responses for the upper  
115 brittle lithosphere (Kohlstedt, et al., 1995). Such frictional behaviors may occur at greater depth,  
116 but only associated with local and transient events (Andersen et al., 2008; Stöckhert, 2002). The  
117 pressure data used by Yamato and Brun (2017) and Bauville and Yamato (2021) were derived  
118 from mineral assemblages that do not represent such events. Tectonic fabrics are common in  
119 (U)HP rocks, as noticed by Bauville and Yamato (2021). They reflect large finite strains,  
120 consistent with viscous flow over the million-year time scale (Kohlstedt, et al., 1995; Jin et al.,  
121 2001). Second, stress state close to the yield state at (U)HP depths requires that GPa-level  
122 differential stresses (up to 2 times the lithostatic pressure) be sustained for the time scale and  $P$ - $T$   
123 condition of (U)HP metamorphism. Such levels of stress are more than an order of magnitude  
124 higher than stress estimates for crustal mylonites (e.g., Behr and Platt, 2014; Stipp and Tullis,  
125 2003) and would have caused (U)HP rocks to flow at strain rates many orders of magnitude  
126 faster than crustal mylonites (Jin et al, 2001; Lu and Jiang, 2019). There is no microstructural  
127 evidence from (U)HP rocks that supports this. Third, because (U)HP rocks are rheologically  
128 distinct bodies constrained at great depth in the lithosphere, the stress orientations and  
129 magnitudes in them are determined by their mechanical interaction with the surrounding  
130 lithosphere (Jiang and Bhandari 2018; Jiang 2016; Eshelby 1957), and are unlikely Andersonian.

### 131 4. Stress, Strain, and Mohr-Coulomb Rheology

132 Bauville and Yamato (2021) have used stress and strain terms interchangeably such as  
133 using “flattening deformation” for a stress state. This would have been acceptable if one deals

134 with elastic-frictional deformation in isotropic materials because in such conditions the strain is  
135 sufficiently small and the principal axes for the stress tensor and for the strain tensor are  
136 coincident. However, the authors propose to use the shape of strain ellipsoid obtained from  
137 tectonic fabrics to determine the relative magnitudes of principal stresses. This ignores the fact  
138 that tectonic fabrics in (U)HP rocks are related to finite strains which accumulate over time in  
139 viscous flows and generally by non-coaxial deformation paths (Means et al., 1980). The strain  
140 ellipsoid from tectonic fabrics do not have any simple relation to the principal stress directions  
141 and relative magnitudes.

142 Yamato and Brun (2017) considered Andersonian stress state only. Bauville and Yamato  
143 (2021) discussed stress rotations at the  $P_r$  stage in Section 3.2 of their paper. The derivation in  
144 this section is sketchy and it is not clear how Eqs.18-20 were derived and then applied to their  
145 Fig.7. One notes that the Mohr-Coulomb plasticity, as a constitutive behavior for elastoplastic  
146 materials, is coordinate system independent. The orientation of the “yield surface” in a Mohr-  
147 circle plot is always measured with respect to the principal stresses. How a rotation of the stress  
148 tensor, which amounts to a coordinate system change, should have any effect on the Mohr circle  
149 location and size is not clear from their paper. The authors may clarify this point by giving more  
150 details of how their Eqs.18-20 were obtained and applied.

151

## 152 **Acknowledgements**

153 The database used in this paper is from Bauville and Yamato (2021) which is already available  
154 from <https://doi.org/10.5281/zenodo.4126862>. I thank A. Yin for reading an early version of this  
155 comment and discussion on buoyancy driving of UHP rock exhumation. Review comments from  
156 John Platt and Stefan Schmalholz are greatly appreciated. Financial support for research from  
157 Canada’s Natural Science and Engineering Research Council (NSERC) through a Discovery  
158 Grant and China’s National Natural Science Foundation (NSRC, grants 41472184 and  
159 41772213) are acknowledged.

160

## 161 **References**

162 Andersen, T.B., Mair, K., Austrheim, H., Podladchikov, Y.Y., Vrijmoed, J.C. (2008). Stress  
163 release in exhumed intermediate and deep earthquakes determined from ultra-mafic  
164 pseudotachylyte. *Geology* **36**, 995–998.

165 Bauville, A., & Yamato, P. (2021). Pressure-to-depth conversion models for metamorphic rocks:  
166 Derivation and applications. *Geochemistry, Geophysics, Geosystems*, **22**, e2020GC009280.  
167 <https://doi.org/10.1029/2020GC009280>

168 Behr, W.M., Platt, J.P. (2014) Brittle faults are weak, yet the ductile middle crust is strong:  
169 Implications for lithospheric mechanics. *Geophysical Research Letters* **41**, 41(22), 8067–8075.  
170 <https://doi.org/10.1002/2014GL061349>.

- 171 Chopin, C. (1984). Coesite and pure pyrope in high-grade blueschists of western alps: a first  
172 record and some consequences. *Contrib. Mineral. Petrol.* **96**, 253-274.
- 173 Ernest, W.G., Hacker, B. R. & Liou, J. G. (2007). Petrotectonics of ultrahigh-pressure crustal  
174 and upper-mantle rocks – Implications for Phanerozoic collisional orogens. *Geol. Soc. Am.* **433**,  
175 21-49.
- 176 Eshelby, J.D. (1957). The determination of the elastic field of an ellipsoidal inclusion, and  
177 related problems. *Proc. R. Soc. Lond. Ser. A, Math. Phys. Sci.* **241**, 376–396.
- 178 Hacker, B.R. & Gerya, T.V. (2013). Paradigms, new and old, for ultrahigh-pressure tectonism.  
179 *Tectonophysics* **603**,79–88.
- 180 Jiang, D. (2016). Viscous inclusions in anisotropic materials: theoretical development and  
181 perspective applications. *Tectonophysics* **693**, 116–142.
- 182 Jiang, D. & Bhandari, A. (2018). Pressure variations among rheologically heterogeneous  
183 elements in Earth’s lithosphere: A micromechanics investigation. *Earth Planet. Sci. Lett.* **498**,  
184 397-407.
- 185 Jin, Z.-M., Zhang, J. Green, H.W., Jin, S. (2001). Eclogite rheology: implications for subducted  
186 lithosphere. *Geology* **29**, 667–670.
- 187 Kohlstedt, D. L., Evans, B., & Mackwell, S. J. (1995). Strength of the lithosphere: Constraints  
188 imposed by laboratory experiments. *J. Geophys. Res. (Solid Earth)*. **100** (B9), 17587–17602.
- 189 Lu, L. X. & Jiang, D. Quartz flow law revisited: the significance of pressure dependence of the  
190 activation enthalpy. *J. Geophys. Res.: Solid Earth* **124**(1), 241-256 (2019).
- 191 Means, W.D., Hobbs, B.E., Lister, G.S., Williams, P.F. (1980). Vorticity and non-coaxiality in  
192 progressive deformations. *Journal of Structural Geology* **3**, 371-378.
- 193 Parrish, R.R., Gough, S.J., Dearle, M.P., & Waters, D.J. (2006). Plate velocity exhumation of  
194 ultrahigh-pressure eclogites in the Pakistan Himalaya. *Geology*, **34**(11), 989-992.  
195 <https://doi.org/10.1130/G22786A.1>
- 196 Powell, R. P. & Holland, T. (2010). Using equilibrium thermodynamics to understand  
197 metamorphism and metamorphic rocks. *Elements* **6**, 309-314.
- 198 Rubatto, D. & Hermann, J. (2001). Exhumation as fast as subduction? *Geology*, **29**(1), 3-6.
- 199 Smith, D. (1984). Coesite in clinopyroxene in the Caledonides and its implications for  
200 geodynamics. *Nature* **310**, 64-644.
- 201 Stipp, M., & Tullis, J. (2003). The recrystallized grain size piezometer for quartz. *Geophysical*  
202 *Research Letters*, 30(21). <https://doi.org/10.1029/2003GL018444>  
203 Stöckhert, B. (2002). Stress and  
204 deformation in subduction zone: insight from the record of exhumed metamorphic rocks. *Geol. Soc. Lond. Spec. Publ.* **200**, 255-274.

205 Yamato, P., & Brun, J. P. (2017). Metamorphic record of catastrophic pressure drops in  
206 subduction zones. *Nature Geoscience*, **10**(1), 46–50. <https://doi.org/10.1038/ngeo2852>